

Rise Or Fall? How Local Factors Influence Coastal Sea Level in The Philippines

*Rosalie B. Reyes¹, Paul Caesar Flores¹, Angela Bauzon¹, Abegail Rediang¹, Rey Mark Alfante¹,
Nikki Alen Pasaje¹, Charina Lyn Amedo-Repollo², Fernando Siringan²,
Ariel Blanco¹, Dennis Bringas³
Marion Ordillano¹, and Pocholo Miguel A. De Lara¹*

¹Department of Geodetic Engineering, University of the Philippines Diliman, Quezon City, Philippines

²The Marine Science Institute, University of the Philippines Diliman, Quezon City, Philippines

³National Mapping and Resource Information Authority
Lawton Ave., Fort Andres Bonifacio, 1634 Taguig City, Philippines

Abstract - The Philippines being an archipelagic country has the fifth longest coastline in the world. Its shores are defined by varying geologic form and composition that defines how sea water could impact its configuration. Being in a tectonically active setting, the country is also affected by ground motion. Specifically, the vertical land motion (VLM) has a significant effect on the observed sea level along the coast. As it is surrounded by large bodies of water, ocean dynamics and climate pattern have also contributed to the variations of sea level. The changing climate altered the global atmospheric pattern that results in varying regional/local effects on the coastal sea level. These local factors are the reasons why sea level varies differently in different places with the global mean sea level (GMSL). This study investigated the coastal sea level trend in 25 out of 50 tide gauge (TG) sites. The observed TG sea level (TGSL) were computed and analyzed for trends. Similarly, sea level trends were also determined from retracked satellite altimeter (SA) products from different satellite missions. The influence of VLM, a non-climatic factor, on the sites were determined using Permanent Scatterer Interferometric Synthetic Aperture Radar (PSInSAR) and validated using data from GNSS (Global Navigation Satellite System) receivers collocated with the TG. The investigation of the occurrence of El Niño was undertaken to explain the computed sea level trend.

Results showed that areas with long period of observations (19 years or more) exhibit an increasing sea level that varies from 1.38 to 13.13 mm/year. However, majority of the TGs that were installed in 2007 and 2008 recorded only 13 and 12 years of observation, respectively. A decreasing sea level trend were observed on said TGs except for those located in Palawan. Similar trends were also observed from sea surface height (SSH) from satellite altimeter. A 0.96 correlation was computed between TGSL and 20 Hz SSH. Investigation showed the strong influence of El Niño during this short period of observation that caused the sea level to fall. The effect of Pacific Decadal Oscillation (PDO) was not analyzed due to limited period of recorded data. The VLM contribution to the observed sea level was determined for 9 sites with collocated GNSS receivers. Most of these sites experienced land subsidence of around -3 to -7 mm/year. The PSInSAR and GNSS VLM rates have a correlation of 0.89. In Manila Bay where sea level rise is accelerating at 13.13 mm/year, one of the contributors is increasing river water loading. However, north of Manila, land subsidence showed 8-12 mm/year rate based on PSInSAR.

Keywords: Coastal Sea Level Rise, Vertical Land Motion, PSInSAR, Satellite Altimetry, GNSS

I. INTRODUCTION

The determination of sea level prior to satellite altimetry was mostly from tide gauges and only near the 1990's, that space technology revolutionized the measurements of sea level remotely with improved accuracy [1]. This has led to estimating the global mean sea level (GMSL) through satellite altimetry [2]. Tide gauges are spatially and temporally limited. Usually, they are installed to service the shipping needs, thus they are located mostly in ports and harbors in inlets for safe anchorage. Location plays a vital role in sea level measurements because this could bias the sea level trend. Factors such as geological setting, geomorphology, ocean dynamics, and other natural and anthropological contributions are site specific. Thus, coastal sea level rise should be treated locally as this varies differently from the GMSL. It is important to focus on local sea level rise because it matters to people living in the coastal areas.

The many factors that influence the local sea level rise contaminates the observed sea level. The response or action to mitigate the effects of rising sea level is determined from the cause. If sea level rise is heavily influenced by land subsidence due to groundwater extraction, then building dikes is not the primary solution. It is also not wise to be safe when the sea level trend shows a fall because this trend can be seasonal. A deeper investigation of contributing factors should be done on areas with accelerating sea level rise to prevent on-going and future infrastructure projects to exacerbate the rising sea level.

The Coastal Sea Level Rise Philippines (CSLR-Phil) Project investigated some of these factors contributing to rising sea level. The objective of the study is to quantify the rate of sea level rise/fall and isolate the contribution of vertical land motion (VLM) that contaminates the sea level observation. It also investigated the influence of El Niño to explain the sea level trend. The determination of the coastal sea level trends at different locations in the Philippines provide local government units (LGUs) with a better way of understanding the rising sea level in their locality. The new estimates could revise their vulnerability assessment and devise a better response to mitigate the effect of rising sea level. The determination of the correlations of TG with SA data and PSInSAR with GNSS data is an important output. The spatial limitation of TG can be complemented by SA whenever available. Also, PSInSAR determined VLM from radar images can substitute for VLM determined through GNSS.

II. MATERIALS AND METHODS

2.1. Study area

To date there are 50 TGs installed by the Physical Oceanography Division (POD) of the Hydrography Branch of the National Mapping and Resource Information Authority (NAMRIA) all over the Philippines. Twenty-five (25) of these were selected for analysis namely: Balanacan, Baler, Batanes, Brooke's Point, Cagayan de Oro, Calapan, Caticlan, Cebu, Coron, Currimao, Davao, El Nido, Guian, Jose Panganiban, Legaspi, Manila, Mariveles, Pagadian, Port Irene, Puerto Princesa, Pulpandan, San Fernando, San Vicente, Tandag and Zamboanga (Figure 1). There are eight (8) sites with collocated GNSS receivers, and these are: Cagayan de Oro, Cebu, Davao, El Nido, Guian, Manila, Legaspi, and San Fernando (highlighted with red triangles) in Figure 1. The 25 sites were decided based on agreement

with the funding agency, with the project doing half of the sites and the POD the other half to capacitate the latter in processing satellite altimeter data.

Among these TGs, six (6) of these have long term observations of 19 years and more. These are Cebu, Davao, Manila, Legaspi, Puerto Princesa and San Fernando. Most of these TGs are installed on pier/wharf and located on ports and harbors that are on indented coastline or inlets intended for navigation operations and not for monitoring sea level rise. The TG location by itself could already influence sea level measurements.

2.2. Data

The data used in this study is listed in Table 1. Most of these are sourced online from data providers and government agencies. The POD NAMRIA provided much of the GNSS field observations on TG Benchmark (TGBM). These were used to transform the Zero Tide Staff (OTS) readings to ellipsoidal heights. A tide staff is a vertical bar graduated in centimeter attached to a pier column near the tide gauge. The zero (0) meter in the tide staff is the reference datum for the sea level measurement. Referring all sea level to one datum facilitates the comparison of sea surface height (SSH) with TGSL. The SSH computed from altimeter data were given in 1 Hz and 20 Hz and retracked using ALES [3], MLE4 [4], [5], and X-TRACK [6].

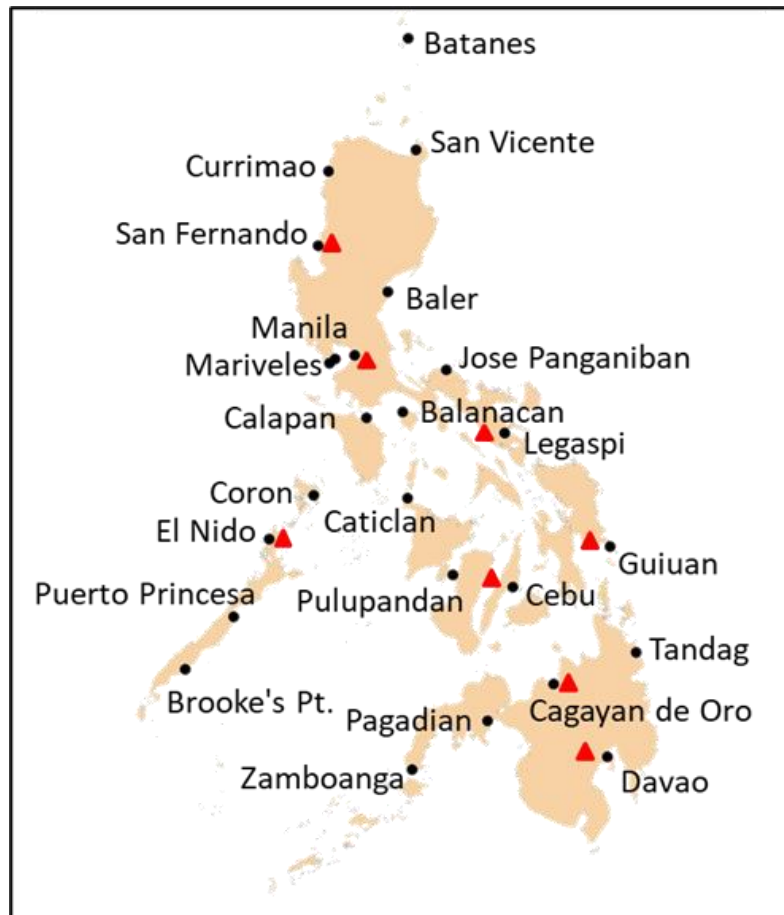


Figure 1. Tide gauge sites (black dots) and collocated GNSS receivers (red triangles)

Table 1. Data Sources

<i>Data Products</i>	<i>Unit of measurement</i>	<i>Data frequency</i>	<i>Data Provider</i>	<i>URL</i>
TG observations	Above OTS in meter	Hourly	NAMRIA	https://www.namria.gov.ph/
CGNSS observations	Ellipsoidal height in meter	Daily solution	NAMRIA	https://www.namria.gov.ph/
AGN observations	-do-	Daily solution	NAMRIA	https://www.namria.gov.ph/
ALES	-do-	1-Hz	OpenADB	https://openadb.dgfi.tum.de/en/
ALES	-do-	20-Hz	PODAAC	https://podaac.jpl.nasa.gov/
MLE4	-do-	20-Hz	AVISO+	https://www.aviso.altimetry.fr/en/
SAMOSAS+	-do-	20-Hz	ESA GPOD	http://gpod.eo.esa.int/
SAMOSAS++	-do-	20-Hz	ESA GPOD	http://gpod.eo.esa.int/
X-TRACK/ALES	-do-	20-Hz	ESA CCI	https://climate.esa.int/en/

The Adaptive Leading Edge Subwaveform or ALES [3] is a new retracking algorithm for determining the sea level for both coastal and open ocean products. The ALES retracker uses part of the returned echo and fits it with the Brown model [7] then convergences through the Nelder-Mead nonlinear optimization technique using least-square estimation [3]. The Brown Model is based on the combined computation of the instrument point target response, flat surface response and probability density function of the specular points [7]. It assumes that beam from the satellite is reflected directly back only at specular points [8].

The X-TRACK data processor [6] was developed to improve both the quantity and quality of altimeter data redefining the data editing strategy to minimize the loss of data during the correction phase and by using improved local modelling of tidal and short-period atmospheric forcing. The processor adopts therefore, new data screening strategy and filtering techniques allowing to recover data that would otherwise be flagged as bad [8].

The Maximum Likelihood Estimator 4 or MLE4 algorithm estimates four parameters: range, significant wave height, power, and the slope of the waveform trailing edge. Although there were drawbacks in the algorithm, MLE4 was adopted for the reprocessing of Jason-1 data and for the subsequent Jason altimeters. Benefits were found using the MLE4 algorithm for the range and significant wave height estimates especially when the return echoes do not conform to the Brown model.

2.3. Method

2.3.1. Determining the rate of relative sea level change

The general method for determining the rates of sea level change from tide gauge and satellite altimeter measurements is shown in Figure 2. An integrated approach was used in this study in quantifying the rate of relative sea level change around the Philippines by using tide gauge measurements complemented by data from satellite altimeter missions such as EnviSat, Jason 1, Jason2, Jason 3, Saral, Sentinel-3A, and Sentinel-3B. The sea level is the height of the

sea surface uninfluenced by wind waves and swell, which is frequently measured relative to a reference horizon [9]. Tide gauge measurements are referred to Zero Tide Staff or OTS which is an arbitrary reference level set at each tide gauge stations. On the other hand, satellite altimeter measurements are referenced to geocentric ellipsoids such as the T/P (Topex/Poseidon) and World Geodetic System of 1984 (WGS84) ellipsoids. It is thus important that the sea level measurements are in the same reference frame to ensure data compatibility.

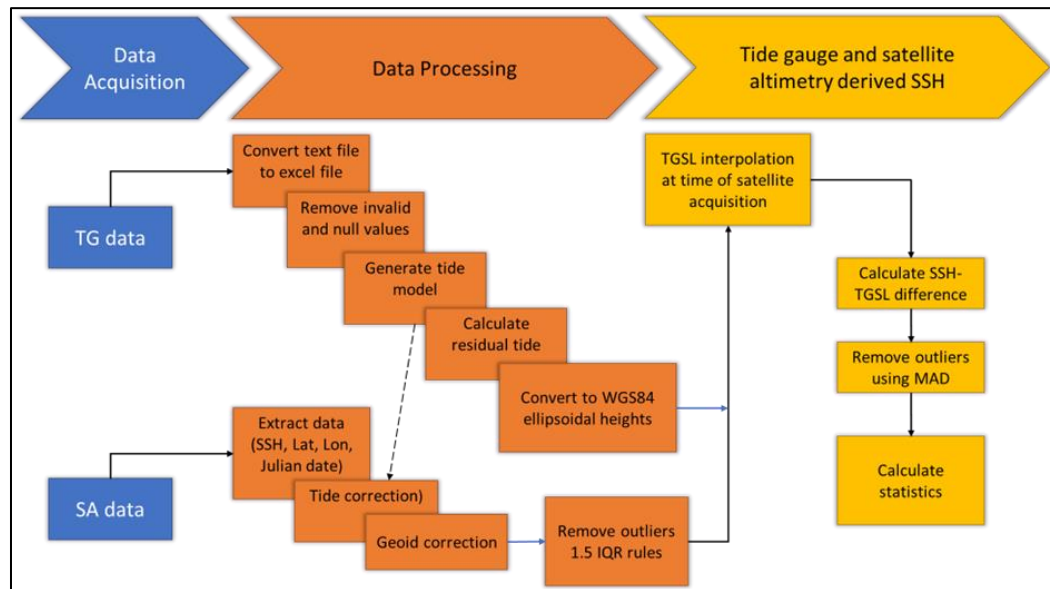


Figure 2. General workflow for determining CSLR/F from tide gauge and altimeter data

2.3.2. Tide gauge processing

The TG measurements were transformed to the WGS 84 ellipsoidal height system so that it will have the same reference datum with the satellite altimeter data. To refer these measurements to WGS84, the nearest tide gauge benchmark (TGBM) was observed with a GNSS receiver to obtain the ellipsoidal height (h_{TGBM}). The height above OTS of the TGBM ($H_{TGBM/OTS}$) is determined through differential levelling. Subtracting these two values converts the OTS to ellipsoidal height h_{OTS} . Shown in Figure 2 is an example of a collocated GNSS-tide gauge station setup. A simple geometric conversion to reference OTS above the surface of an ellipsoid (h_{OTS}) is:

$$h_{OTS} = h_{TGBM} - H_{(TGBM/OTS)} \quad (\text{Eq. 1})$$

To convert the TGS measurements into ellipsoidal heights, the hourly tide gauge readings are then added to the value of the h_{OTS} . Therefore:

$$\text{Ellipsoidal height of TGS} = h_{OTS} + \text{hourly TG readings} \quad (\text{Eq. 2})$$

2.3.3. Satellite altimetry processing

Satellite altimeters provide range measurements and must be converted to sea surface height (SSH) following the general equation [10]:

$$SSH = \text{satellite altitude} - (\text{measured range} + \text{geophysical corrections}) \quad (\text{Eq. 3})$$

Geophysical corrections include inverse barometer pressure, sea state bias, ionosphere correction, ocean tide, polar tide, Earth tide, wet tropospheric correction, and dry tropospheric correction. Since satellite altimeter measurements are degraded near the coasts due to contamination of land masses [7], this study utilized retracked satellite altimeter datasets because of the improved quality near the coast. The SSH measurements for each tide gauge station were only limited to satellite passes that are within 3 to 50 km radius from the tide gauge. The 50-km radius was adopted from Coastal and Hydrology Altimetry product (PISTACH) handbook [10], where data from satellite altimetry can still be effectively compared. The less than 3 km distance to coast data exclusion was based on the threshold recommended by OpenADB [11].

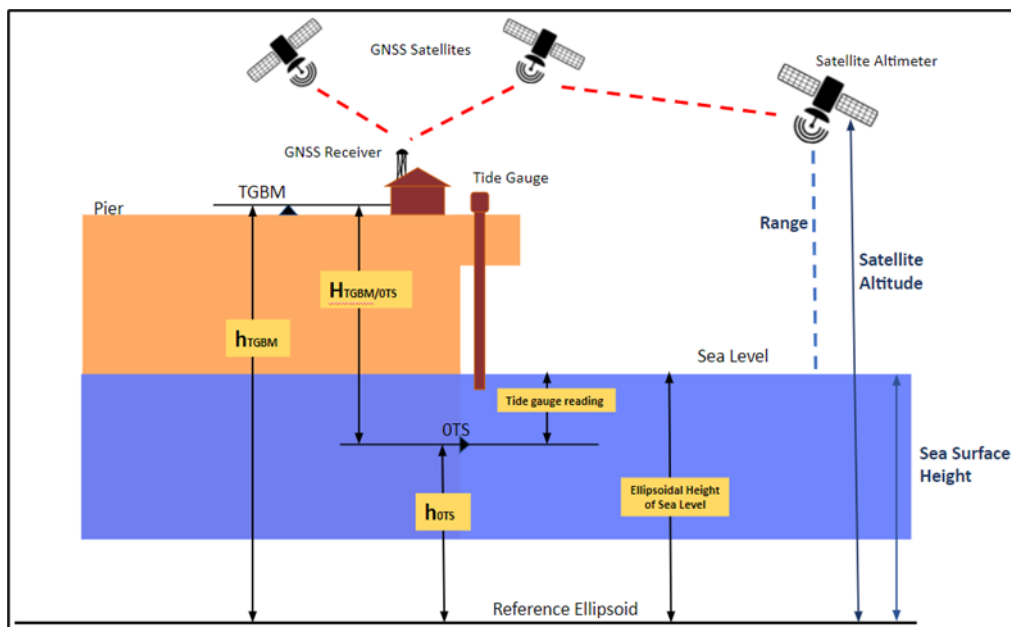


Figure 3. Schematic representation of a collocated GNSS receiver with tide gauge station

2.4. Determining vertical land movement

Three (3) methods are presented herein for determining VLM: (1) SSH-TGSL difference, (2) GNSS solutions, and (3) PSInSAR. The same methods were also used by Grgić et al., [12] for determining VLM in the Dubronik area in Croatia. The difference is that said study used only the images of Sentinel-1 in ascending orbit while this study considered the ascending and descending (AD) pair of images for processing. Figure 3 shows the workflow for VLM determination.

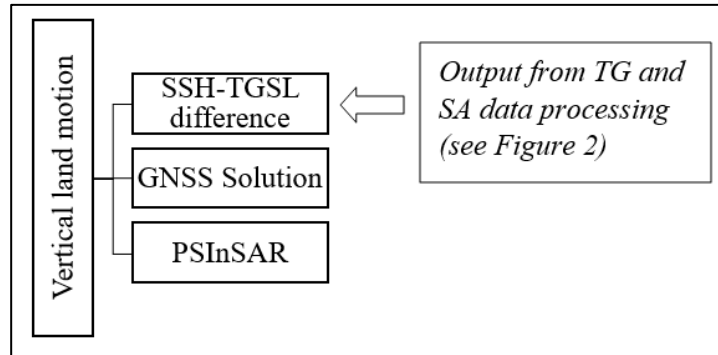


Figure 4. VLM determination workflow

2.4.1. SSH-TGSL difference

The VLM can be inferred or estimated by taking the difference between SSH derived altimeter measurements and TGSL. This approach was utilized to provide estimates for VLM in some studies [13], [14], [15] mainly because tide gauges are affected by VLM while satellite altimeters are not. Thus, the difference between TGSL and SSH should, in theory, provide a reliable estimate for VLM.

Since the acquisition time for the satellite altimeter data differs from the tide gauge observation time, cubic interpolation [16] was performed on the hourly tide gauge measurements of NAMRIA to estimate the TGSL at the time of satellite acquisition. Other types of interpolation were tested for tide gauge data estimation, but cubic interpolation produced the best fit to the actual data used for validation. The estimated rate of VLM is then given by the difference between TGSL and SSH.

2.4.2. GNSS solutions

Continuous GNSS data gathered from NAMRIA's collocated GNSS receivers at the tide gauge stations were post-processed through AUSPOS [17] of Geoscience Australia. Post-processed daily solutions of GNSS data were computed and filtered to eliminate outliers. The daily solutions were plotted in time-series for each GNSS station to analyze the trend. The trend lines in the plot represent the vertical velocity of local land motion at GNSS station near the TG within the period covered by the GNSS dataset. An example of the GNSS plot in Manila GNSS station is shown in Figure 5.

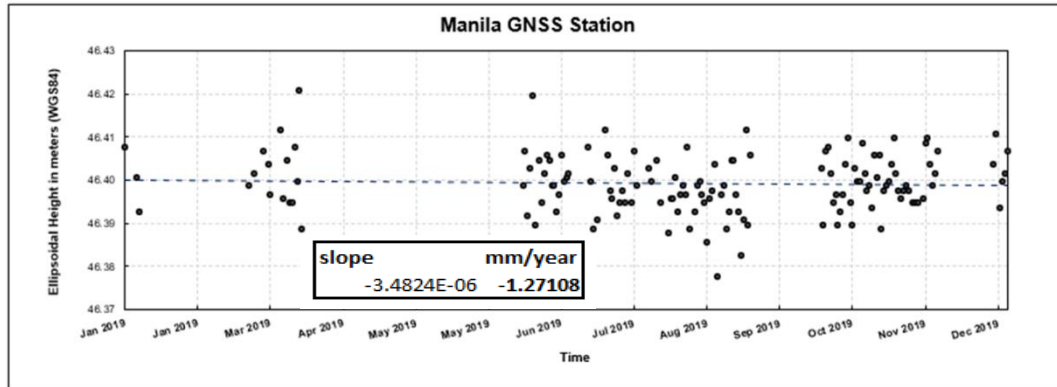


Figure 5. Plot of GNSS solutions in the vertical direction

2.4.3. PSInSAR

The PSInSAR is a method that utilizes radar satellite images to determine temporal vertical land movement. This method identifies points whose response to the radar is dominated by strong reflection and is constant over time. These points are called permanent scatterer or PS points. In this study, the implementation of this method is limited only to TG sites with GNSS receivers. This is to ensure that there is an independent data to validate the results of PSInSAR. Single Look Complex (SLC) Sentinel-1 radar images were downloaded from the Alaska Satellite Facility (ASF) Vertex [18]. For each ascending/descending flight directions, at least 20 images with, ideally, 12 to 24-day interval were downloaded per site to obtain reliable PSInSAR results. Processing was entirely implemented in SARPROZ [19], a software that offers SAR, Interferometric SAR, and Multi-temporal InSAR processing techniques.

Two SARPROZ modules were mainly used in permanent scatterer selection namely, 1) Atmospheric Phase Screen (APS) Estimation and (2) Sparse Point Processing. The APS Estimation mainly retrieves and removes the influence of atmospheric delay in the datasets which could result to radar signal delays. PS points were firstly filtered based on the amplitude stability index (ASI), with the threshold ranging from 0.7 to 0.85 depending on the site's land cover and sparsity of persistent scatterers. This threshold determines the initial number of points to be analyzed. The creation of a connection graph using Delaunay triangulation followed, along with setting other processing parameters. For PSInSAR, a stable reference point is used to determine line of sight (LOS) land movement. However, due to the unavailability of a stable GNSS base station in all sites excluding Manila, a suitable reference point based on phase stability and high temporal coherence was selected per site. Graph inversion was then implemented to finally remove atmospheric delay in the dataset and overall temporal coherence in the site was analyzed. The same parameters were used to the Sparse Point Processing module to select second order PS points and to generate a time series file. Vertical velocity was lastly obtained by analyzing both ascending and descending LOS displacements using the AD pair method in the Multi-Sensor Module. The vertical velocity recorded by the nearest PS point to the tide gauge is used to observe and validate vertical land movement observed in the area.

III. RESULTS AND DISCUSSION

3.1. Calculated rates of sea level rise/fall (SLR/F) from tide gauge stations

The calculated rates of sea level rise/fall from tide gauge stations are shown in Table 2 and Figure 6. The SLR rates computed from Batanes, Calapan, Mariveles and Jose Panganiban are dubious due to many gaps in the observations. For sites with long term observations (19 years and more) such as Manila, Cebu, Puerto Princesa, Davao, and Legaspi, the SLR rates are on the rise except San Fernando. The reason for the latter is the many data gaps due to constant malfunctioning of the TG sensor. Manila has the largest SLR rate at 13.13 mm/year from 1970 to 2020. The sea level is falling for TG sites with short period of observations (12 and 13 years except for those in Palawan. These TGs were installed in 2007 and 2008 and these are Baler, Cagayan de Oro, Caticlan, Currimao, Guiuan, Pagadian, San Vicente, Tandag and Zamboanga. Observation in Port Irene was discontinued until 2006 because it was transferred to San Vicente, Cagayan. Note that Port Irene although located near San Vicente exhibit SLR trend opposite the SLF trend in San Vicente. This is because of the different period of observations. The TG sites in Palawan namely Brooke's Point, Coron and El Nido have a positive SLR rates that indicate a rising sea level.

Other than the period of observations affecting the SLR trend, location of TGs also influenced the observed sea level. Those TGs located in the east (facing Pacific Ocean), north and south of the country exhibit sea level fall. In later discussion this will be elaborated. The Palawan TGs are facing the West Philippine Sea and are on the rise. The TGs located on islands in the interior waters of the Philippines such as Balanacan, Caticlan, Pagadian and Pulpandan have varying sea level trend. Caticlan and Pagadian exhibit sea level fall while Balanacan and Pulpandan a sea level rise.

The Manila Bay sea level trend was derived from 1970 to 2020 observations in the Port Area TG. This is the period where an uptrend was observed. Data from TGs along the Manila Bay such as Limay and Mariveles in Bataan were investigated to determine if same trend is being observed. However, Limay data is erratic and full of data gaps due to numerous sensor breakdowns. Mariveles TG is near the mouth of the bay but also experience the same problem with Limay TG. Thus, sea level trend observed at Manila Port Area TG was not verified from nearby TGs in the bay. Validation of the sea level trend was retracked satellite altimeter data.

3.2. Calculated rates of SLR from along track satellite altimeter retracked products

Several retracked along track altimeter products were used to determine the SLR rates and trends in the sites where TGs were installed. These were from ALES 1 Hz and 20 Hz, XTRACK-ALES 20 Hz, and MLE4 20 HZ retrackers. SAMOSA+ and SAMOSA++ retrackers for Sentinel-3 altimeter products were also done but have poor results. On average, the standard error was 4.52 m in comparison with the tide gauge data, hence was excluded in the analysis. The four years of satellite altimeter measurements from Sentinel-3 were very short to achieve good estimates of sea level trend.

Only 8 of 25 sites have available ALES 20 Hz retracked product. These data were mostly from 2008 to 2015. The computed rates from Balanacan, Batanes, Currimao, Guiuan, San Fernando, Tandag and Zamboanga have falling sea level that varies from -6.38 to -14.03

mm/year. Pulupandan SLR rate is dubious because of too many data gaps and short period of observations.

Table 2. SLR/F rates calculated from TG data

<i>Site</i>	<i>Period</i>	<i>Rate (mm/yr)</i>	<i>Std err</i>
Balanacan	2007-12 to 2020-12	0.12	0.64
Baler	2010-05 to 2020-07	-11.80	0.90
Batanes	2017-01 to 2020-12	<i>Too many data gaps</i>	
Brooke's Pt.	2008-01 to 2020-09	8.17	5.19
Cagayan de Oro	2007-10 to 2020-12	-1.05	0.49
Calapan	2009-08 to 2015-12	<i>Too many data gaps</i>	
Caticlan	2008-03 to 2020-11	-2.67	0.55
Cebu	1947-05 to 2020-12	1.28	0.04
Coron	2008-03 to 2020-12	7.53	0.55
Currimaos	2007-11 to 2020-11	-10.02	0.29
Davao	1948-03 to 2020-12	3.14	0.06
El Nido	2014-01 to 2020-12	9.91	1.05
Guiuan	2008-01 to 2020-12	-5.76	0.31
Jose Panganiban	2011-01 to 2020-11	<i>Too many data gaps</i>	
Legaspi	1948-02 to 2020-12	5.56	0.06
Manila	1970-01 to 2020-12	13.13	0.05
Mariveles	2002-01 to 2016-11	<i>Short period of observations</i>	
Pagadian	2011-01 to 2020-12	-6.84	1.09
Port Irene	1987-02 to 2006-12	7.01	0.27
Puerto Princesa	1990-07 to 2020-09	6.19	0.30
Pulupandan	2013-01 to 2020-12	4.70	0.14
San Fernando	1988-01 to 2020-12	-1.01	0.10
San Vicente	2007-11 to 2017-11	-7.81	0.97
Tandag	2008-02 to 2016-12	-5.64	1.20
Zamboanga	2008-01 to 2020-12	-14.20	0.38

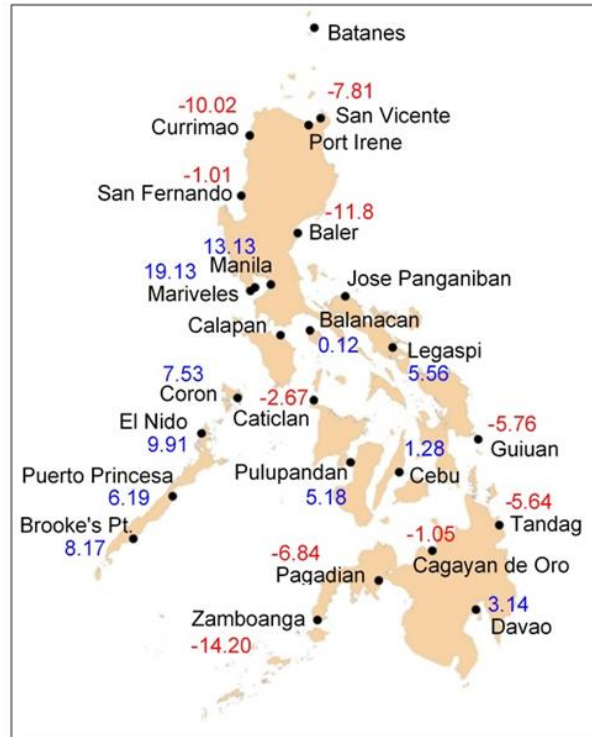


Figure 6. SL rise (blue) and fall (red) rates from TGs

The XTRACK-ALES retracked product were only available at 8 sites. The periods of observations were mostly from 2002/2003 to 2018 for Balanacan, Currimao, Guiuan, San Fernando and Zamboanga. All the computed sea level rise rates from these sites are on the rise with rates from 1.65 to 2.69 mm/year. Batanes, Tandag and Pulupandan have doubtful results.

Among the 20 Hz retracked products, MLE4 has 80% of the sites with data availability. Sites with no data are Cebu, El Nido, Legaspi, Paqadian and Puerto Princesa. Observations with almost 19 years of data are Balanacan, Currimao, Guiuan, San Fernando and Zamboanga. Except for Guiuan these sites have sea levels increasing. The remaining sites have observations from 2008 onwards that show varying sea level trends. Baler, Brooke's Point, Calapan, Davao and Tandag computed SLR/F rates are questionable. These are again due to data gaps. Manila sea level is only around 3.65 mm/year from 2008 to 2018 while Mariveles has 9.68 mm/year from 2009 to 2019.

The comparison of TGSL and SSH 20Hz was made for the same period of observation. The period considered was from 2008 to 2020 where most 20 Hz data were available. The SA SLR rates were mostly from MLE4 but also incorporates results from ALES and XTRACK whenever these performs better than MLE4. Figure 7 summarizes the rates from TG and SA data. It can be observed that both datasets show the same trend for most of the TG sites compared. Those sites located in inlets and inland waters deviates much from each other due to the altimeter signal contamination of the surrounding land masses.

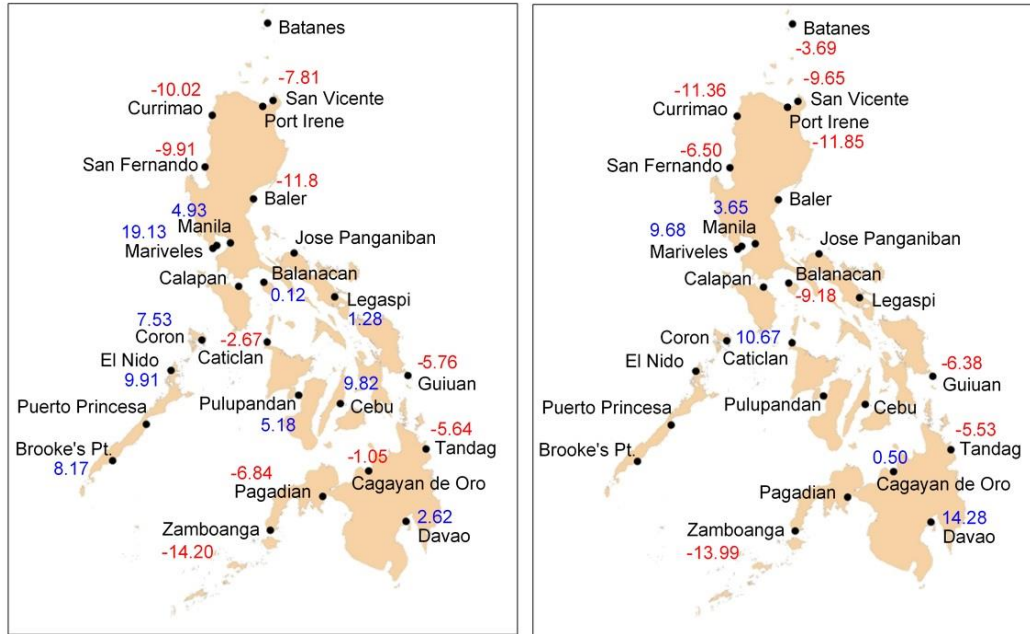


Figure 7. Comparison of TG (left image) and SA 20 Hz (right image) derived SLR/F rates from 2008 to 2020. Red indicates sea level fall and blue sea level rise

The ALES 1 Hz had the longest data that spans 18 years (2002-2019) for most of TG sites. No SLR rates were determined for Cebu, El Nido, Legaspi, Pagadian and Puerto Princesa due to unavailability of data. The SLR trend from this data is mostly on the rise with high estimate in Jose Panganiban site at 9.19 mm/year. The nearby site in Baler also showed a high rate of 7.33 mm/year. Like TG measurements the altimeter showed sparse data in these sites. Batanes has a high SLR rate of 8.35 mm/year that could be due to short period (9 years) of observations. Davao has also sparse data that results in 8.30 mm/year SLR rate. The negative trend in Brooke's Point is due to 1 year of available data. Manila sea level also exhibited a downtrend because the altimeter data has few processed points at 1 Hz compared to 20 Hz data.

The limitation of point measurements from along track altimeter products is overcome by the gridded products. The said product was a result of interpolation of point measurements from along track altimeter observations. Void spaces or areas with no data were filled up with data due to interpolation. The biggest advantage of this gridded data is the long period of assimilated data from satellite altimetry that started in 1992. The MEaSUREs Gridded Sea Surface Height Anomalies Version 1812 [20] was used for extracting the sea level anomalies. Based on the product document the accuracy is around 7.5 cm validated from 61 tide gauges all over the world. However, users are cautioned in its use because no detailed assessment was done near coasts [20]. The sea level trends from this product for all sites are positive or increasing. Interestingly, Manila and Mariveles SLR rates are 3.85 mm/year and 3.64 mm/year, respectively, that are almost the same. The sea levels in Davao, Tandag, Baler and Guiuan exhibit the highest rates ranging from 6.98 to 10.01 mm/year.

The two datasets (ALES 1Hz and MEaSUREs) with long period of observations were also compared and the summary is shown in Figure 8. Both products showed an uptrend and the

values do not differ much. The values in black are the rates computed from TGs for the same period. The TG rates have large disparities with SA rates except for Puerto Princesa site. The rates from neighboring sites usually exhibit homogeneity excepting Baler and Jose Panganiban. Even TG measurements from these sites were very erratic due to the presence of eddies in the area.

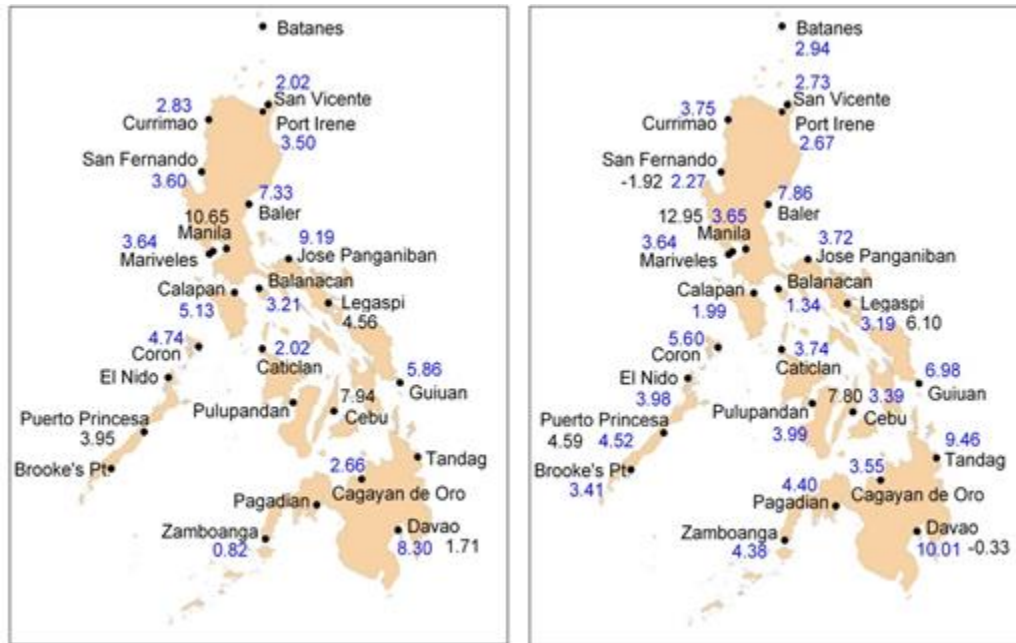


Figure 8. Comparison of ALES 1 Hz (left image) and MEaSUREs (right image) derived SLR/F rates

3.3. The influence of El Nino in the observed sea level

As was explained in the previous discussion, the length and period of observations greatly affect the SLR rates and trend. Here, the length of observation refers to the duration of observation or specifically the number of years of sea level measurements. The period as used in this study refers to a specific or definite interval between points of observation at a defined time. Most of the TGs maintained by NAMRIA were installed in 2007 and 2008. The period starting from the first acquisition up to the year 2020 can be considered short for sea level rate and trend determination. This is because influence of the ocean-atmosphere climate variability such as the Pacific Decadal Oscillation (PDO) can only manifest in long term observations of 50 years or more [21]. The El Niño event occurs every 2 or 7 years [22], hence short period of observation will not reveal the true sea level trend due to its influence. The observed sea level behavior varies with the duration of occurrence and strength of El Niño.

The period of observation between 2007 and 2020 is dominated by the El Niño in 2009-2010 and 2015-2016. The occurrence specifically in 2015 to 2016 is one of strongest in the historical record [23]. El Niño is associated with warm temperature, thus expanding the water resulting in higher observed sea level [24]. However, this occurs in the central and eastern Pacific. During this time, trade winds in the Pacific weakens, hence preventing the warm water

to travel westward to the Philippines coasts. Thus, while the eastern Pacific is experiencing higher sea level, the coastal water in the Philippines is falling. This is the reason why the observed sea level for most TGs showed sea level fall specifically those facing the Pacific Ocean, Luzon Strait and Mindanao Sea. The same trend were observed by altimeter sensors for the period 2007 to 2020.

The TGs in Palawan showed an opposite trend which is in an uptrend for the same period of observations. One of the reasons is that during El Niño increased water flow westward in Luzon Strait (north of the Philippines) but the buoyant surface water from the West Philippine Sea blocks tropical Pacific surface water injection from the Mindanao Retroflexion (Figure 7) [25]. Thus, water in the South China Sea (SCS) is warm and when southwest monsoon or “Habagat” comes, it warms the water more because it pushes warm water from south and across the SCS to Palawan. Along with warm water, this monsoon also accumulates water on the Palawan side, both contributing to the increase in the sea level (C. Repollo, personal communication, October 7, 2021).

3.4. Comparison of retracked SSH and TGSL

The comparison between SSH and TGSL was done by time-collocating the data. The TG data was interpolated to match the altimeter measurement at that time of acquisition. Basically, the amount of data for analysis depends upon the number of matched points between datasets. The period of observations is also matched. If there are data gaps in the TG data, the SA data even if available, will be voided for that period and vice versa.

The ALES 1 Hz biggest drawback is the data frequency. Only few data can be time collocated with the TG data for comparison. Additionally, most of the TGs have short period of observations. With limited data, the computed SLR rates from the two datasets have poor agreement. Since tide gauge observations are dense and harmonic in nature, matching with sparse altimeter data cannot provide good comparison. In this case, the match points between datasets were determined from the number of altimeter data points and were the basis for computing the statistics. The sites that have a matched period (2002-2019) were Davao and San Fernando. Cebu and Legaspi have no available SA data. SA data for Manila for this retracked product started in 2009. Still the comparative results based on statistics are poor. On average the mean difference between the datasets is around 5.29 cm, standard deviation is 39.55 cm and correlation is 0.66. Nevertheless, the ALES 1 Hz product due to its almost 19 years of data is advantageous for sea level rate and trend analysis.

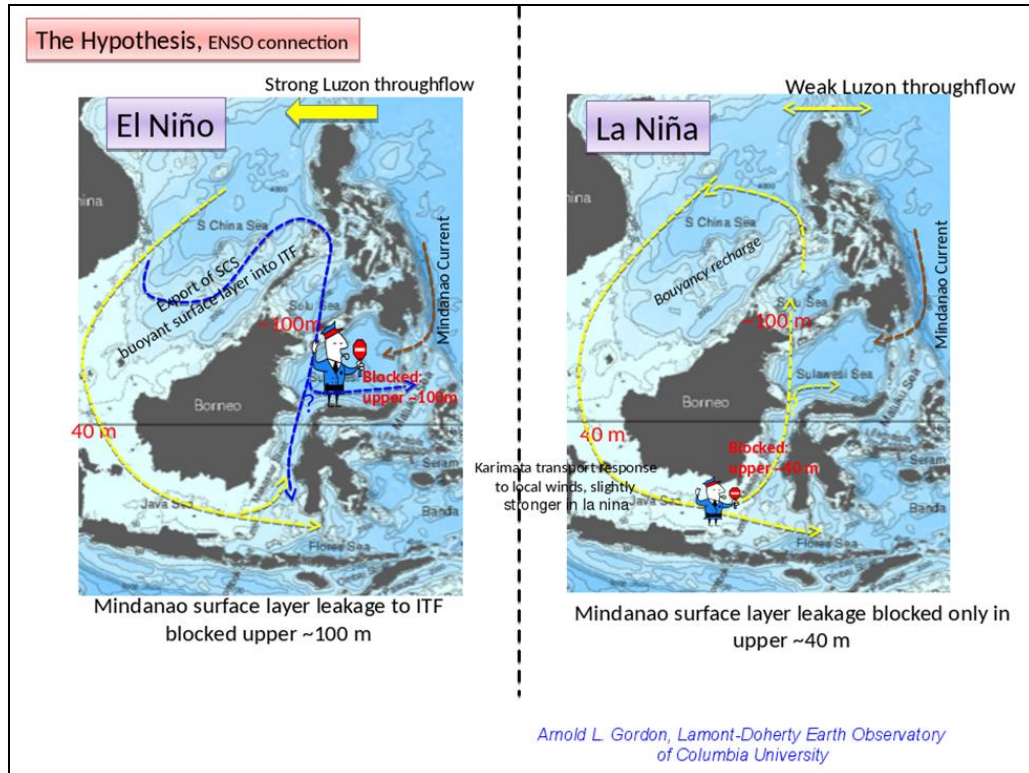


Figure 9. The El Niño connection [25]

The comparison between ALES 20 Hz SSH and TGSL was made on 7 TG sites (Balanacan, Currimao, Guiuan, Pulpandan, Tandag, San Fernando and Zamboanga). The only limitation of this product is the short period (2008-2015) of data availability. However, the comparative results are good except for Pulpandan and Zamboanga. For some areas, the correlations are high, but the offsets are big. This could be attributed to some error in the leveling or the data itself. Pulpandan TG is facing a narrow channel between Negros and Guimaras islands. For satellite altimetry this is disadvantageous because the radar backscatter is degraded by the signals from the landmasses. The big offset in Zamboanga site may be due to error in TGBM elevation or GNSS observed height. The average mean difference between SSH and TGSL for all sites is 3.65 cm excluding Pulpandan. The average standard deviation and correlation are 11.96 cm and 94%, respectively.

Data availability of XTRACK-ALES and TGSL are for the same 7 TG sites as above. However, the periods of SA data start vary from 2002 to 2008 and data end vary from 2016 to 2018. San Fernando has the longest matched period (17 years), hence gave the smallest mean difference of 1.57 cm. This product also showed Pulpandan and Zamboanga sites as problematic. The correlation between the XTRACK-ALES and TGSL data is high at an average of 95%. The average mean difference and standard deviations are 10.81 cm and 12.60 cm, respectively. Pulpandan data is excluded in the statistical results.

The retracked SA data using MLE4 covered 14 TG sites with varying period of data availability. San Fernando again has the longest matched period of 19 (2002-2020). Balanacan,

Davao, Jose Panganiban, Manila, Pulupandan, and Zamboanga have questionable results. Again, for most of these sites the problem is the presence of land masses in the surrounding. Excluding only Pulupandan, the average mean difference is 2.06 cm that is better than the other 20 Hz retracked products. The average standard deviation is 11.56 cm and a high correlation of 97%.

The comparison between the SA retracked SSH and TGSL is summarized in Table 3. Based on the Criteria for comparison [25], the mean difference should be ≤ 12 cm and the standard deviation should be ≤ 10 cm. The 20 Hz retracked products have a high correlation with the in-situ TG data and acceptable mean difference albeit the standard deviation is a little more than the set criteria. Due to its high correlation SA data (wherever available) can be used in areas where no TGs are installed.

Table 3. Summary of comparison of retracked SSH and TGSL

<i>SA Products</i>	<i>Mean Diff (cm)</i>	<i>Mean Std Dev (cm)</i>	<i>Mean RMSE (cm)</i>	<i>Mean Correlation</i>
ALES 1 Hz	5.29	39.55	42.58	0.66
ALES 20 Hz	3.65	11.96	15.81	0.94
XTRACK 20 HZ	10.81	12.60	15.99	0.95
MLE4 20 Hz	2.06	11.56	17.50	0.97

3.5. Vertical land motion

Taking into account the VLM's contribution to the observed sea level is important because in some areas the VLM rate is larger than the SLR rate. The sea level may appear increasing because the land is subsiding and vice versa. Three methods were used for the determination of VLM rates namely: PSInSAR, GNSS solution and SSH-TGSL difference. There are 9 sites that were analyzed for VLM: Balanacan, Cagayan de Oro, Cebu, Davao, El Nido, Guiuan, Lagaspi, Manila and San Fernando. The selection was based on the availability of Continuous GNSS (CGNSS) receiver at the site. Balanacan has no CGNSS, but an Active Geodetic Network (AGN) Station nearby was used. The line of sight (LOS) from PSInSAR was validated using data from said AGN station. Then the correlation was computed to determine the usability of PSInSAR computed VLM rate near the TG site.

3.5.1. Calculated VLM rates from PSInSAR

The rates of vertical land movement (VLM) at the 9 sites were based on the values of the nearest PS from the tide gauges (Table 4) [26]. The assumption is that the nearest PS due to proximity will have the same VLM rate at the TG site. The distances of these PS were limited to less than 1 km. All sites are undergoing land subsidence except for Legaspi site are undergoing land subsidence. Cagayan de Oro and El Nido have high VLM rates of -6.80 and -5.20 mm/year, respectively. An example of the generated vertical velocity map for Manila and vicinity is shown in Figure 7. The area was limited to just around 20 km from the Manila Bay TG. North of Manila the areas along the coast are undergoing land subsidence. These findings agree with the results by Deguchi et al. [27], INDRA and GISAT [28].

3.5.2. Comparison of VLM rates from GNSS and PSInSAR and SSH-TGSL

The comparative results of VLM rates from the three methods are summarized in Table 5. There is no collocated CGNSS receiver in Balanacan site. Thus, the data from AGN station in Moggog that is 6 km away from the TG was used to validate the VLM rate derived from PSInSAR using the nearest PS point [29]. Figure 8 shows the VLM derived rates from the GNSS and PSInSAR solutions. After determining the similarity of VLM rates from the two datasets at the AGN site, the VLM rate at Balanacan TG site was decided using PSInSAR. From Table 5 it can be seen the small differences between PSInSAR and GNSS rates. The correlation between these 2 datasets is 0.89. With this high rate of correlation, it can be concluded that PSInSAR can be used sans availability of GNSS receiver in the site. The SSH-TGSL difference have similarity with PSInSAR and GNSS in the San Fernando and Guian sites. The limitation of SA is apparent in areas where sites are surrounded by nearby landmasses (e.g., Manila and Balanacan). In most cases, this method can be used to indicate the occurrence of vertical land motion. Depending on the data density, this could also provide better estimate of VLM.

Table 4. VLM (mm/year) rates from PSInSAR [26].

Site	Period	Distance of nearest PS from TG (m)	VLM rate (mm/year)
Balanacan	2016-12 to 2019-12	680	-3.90
Cagayan de Oro	2018-01 to 2019-12	354	-6.80
Davao	2016-12 to 2019-12	300	-1.40
El Nido	2017-10 to 2020-12	183	-5.20
Guiuan	2017-08 to 2019-12	375	-1.40
Legaspi	2019-01 to 2020-12	256	0.70
Manila	2017-05 to 2019-12	305	-1.40
San Fernando	2017-08 to 2019-01	165	-1.10

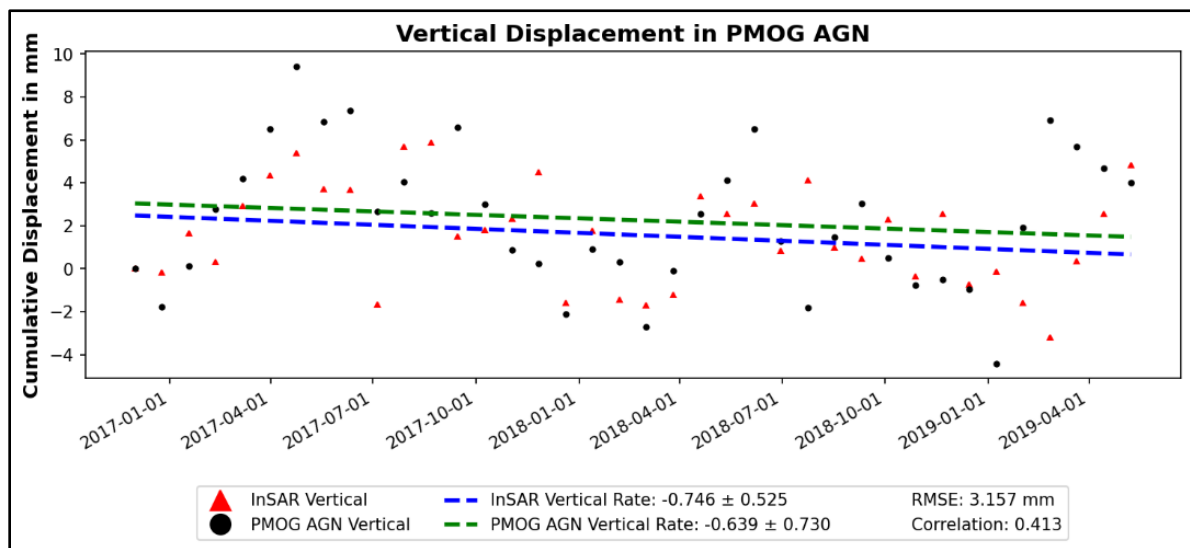


Figure 10. Vertical velocity rates from PSInSAR and GNSS solutions.

3.6. The Manila Bay SLR

Interestingly, the common attribution of Manila SLR is due to land subsidence. However, several studies [26], [27], [28], [30], [31] showed that land subsidence is mostly occurring north of Manila, specifically in Caloocan, Malabon, Navotas and Valenzuela or known as CAMANAVA area. Near the Manila Bay TG land subsidence is very minimal, which means that the TG is recording an accelerating sea level increase not because of ground subsidence in the TG site. This means that other contributing factors are influencing the observed sea level rise. In the initial results of the hydrologic modeling conducted by Herrera [32] for the IM4ManilaBay Project, there was an increase in the discharges from 2004 coming from the different river basins surrounding Manila Bay (Figure 8). The 1988 result is unreliable since the resolution of the satellite images used was very coarse. Due to changing land cover/land use, an increase in surface run-off was also observed. The possibility of continuous land reclamation in the coastal areas may also contribute to SLR. A thorough study regarding the direct influence of land reclamation should be conducted as this is a continuing activity.

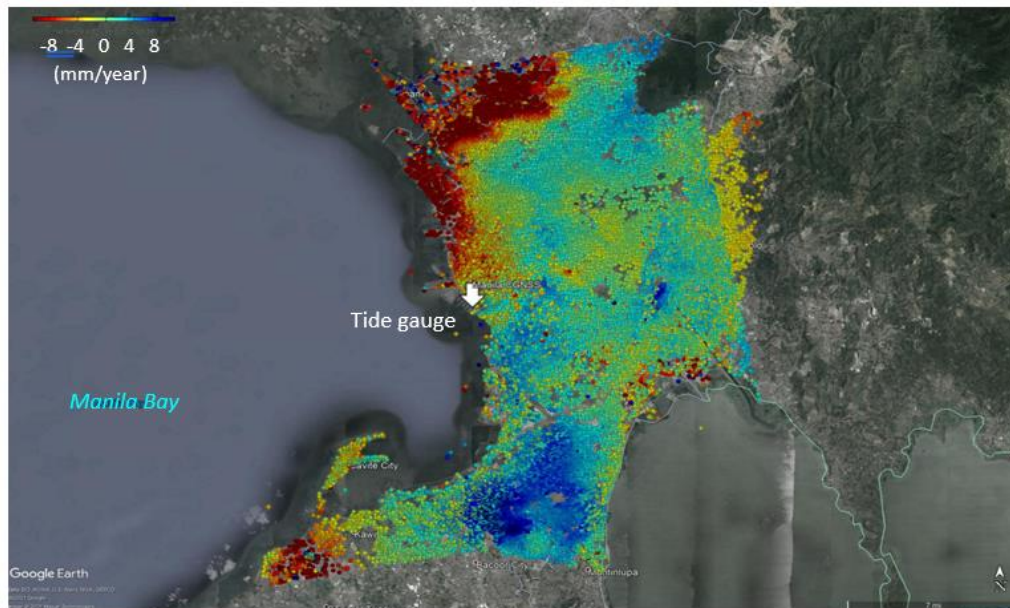


Figure 11. Vertical velocity rates within 20km radius from Manila TG

Table 5. Comparison of VLM rates from PSInSAR, GNSS and SSH-TGSL difference

<i>Location</i>	<i>PSInSAR</i>	<i>CGNSS at TG</i>	<i>SSH-TGSL</i>
Manila	-1.40	-1.00	-4.36
San Fernando	-1.10	-0.62	-1.65
Cagayan de Oro	-6.80	-5.43	Many data gaps from SA
Balanacan	-3.90	No CGNSS on site	-9.06
Guiuan	-1.40	-0.91	-1.35
Cebu	-0.90	-1.11	No satellite pass
El Nido	-5.20	-5.20	No satellite pass
Davao	-1.40	-1.59	Many data gaps from SA

An increasing temperature can cause water to expand thus cause SLR. Figure 10 shows the daily sea surface temperature (SST) from Group for High Resolution Sea Surface Temperature (GHRSS) [33]. Data sources are from satellites with infrared imagers and microwave sensors. It also includes data from drifting buoys, vertical profiling floats, or deep thermistor chains. From 2002 to 2020 the daily SST is increasing at 0.031°C/year. The Physical Oceanography Division (POD) of the NAMRIA measured the sea water temperature and density in 2002 and 2003 but it was discontinued. Measurements resumed in 2018 and on-going. From 2002 to 2020 the water temperature near the TG showed an increasing trend with a rate of 0.09°C/year (Figure 10). For the same period, the rate of SST from GHRSS model is 0.01°C/year. The measured density of sea water is also showing a decrease of 0.385 ppt/year (parts per thousand per year) (Figure 11). These readings can also explain the increasing sea level in the bay.

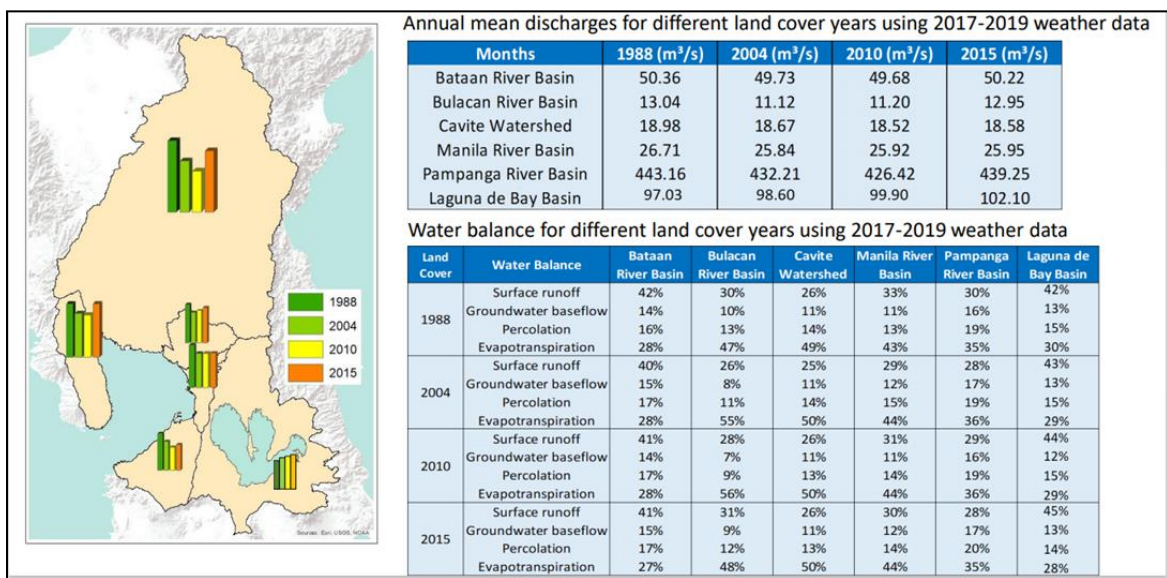


Figure 12. Annual mean discharges from rivers basins around Manila Bay

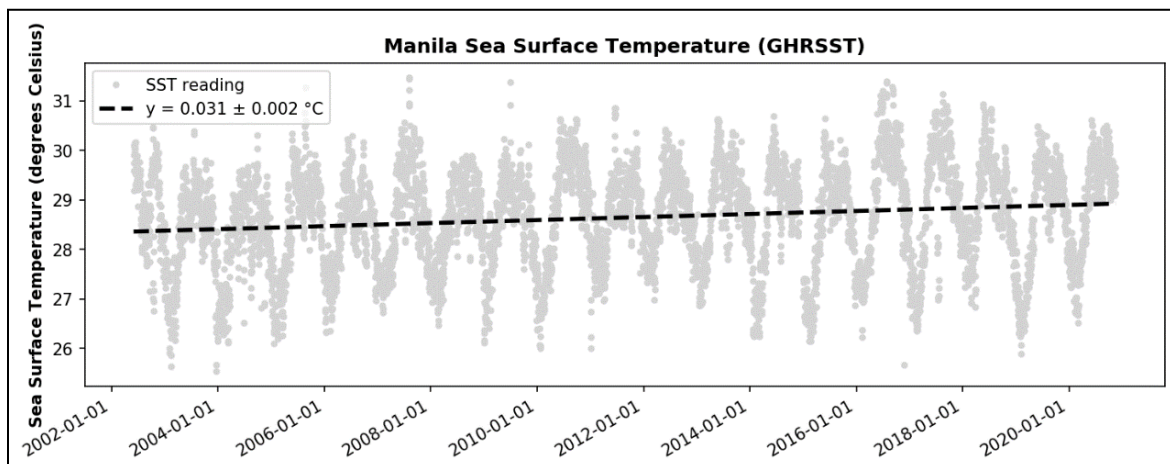


Figure 13. Sea surface temperature trend in Manila Bay from GHRSS

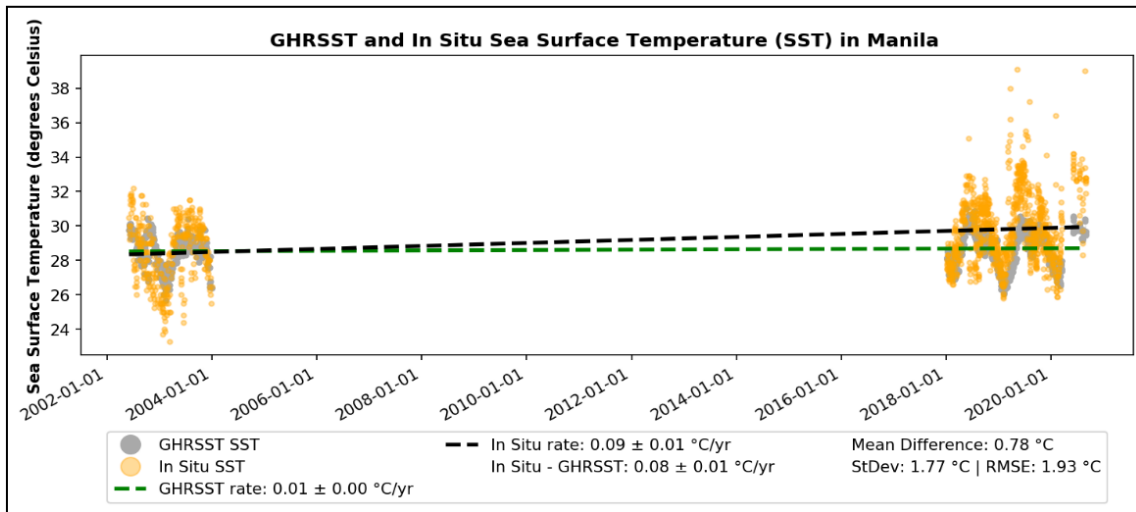


Figure 14. Comparison of GHRSSST and in-situ SST measurement

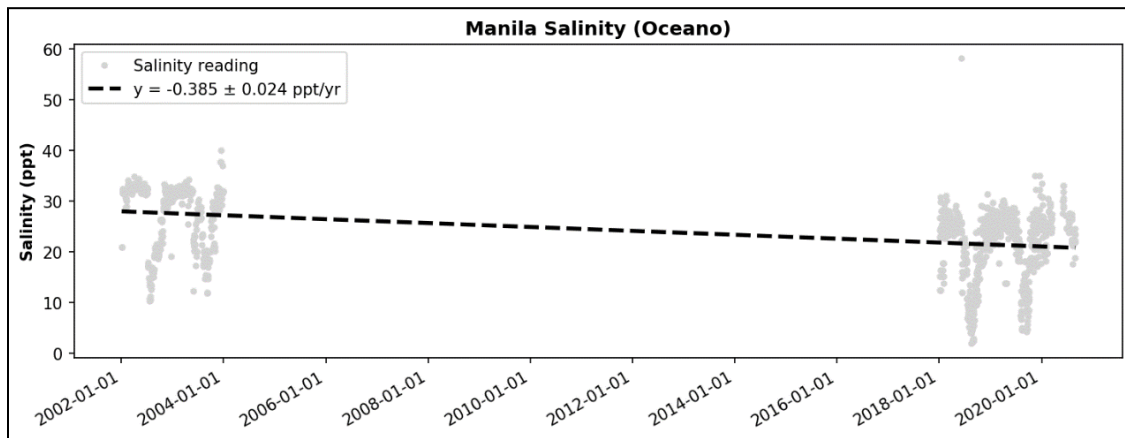


Figure 15. Trend of in-situ measured salinity

3.7. Net sea level rise

The net SLR can be determined by isolating the contribution of the non-climatic factor VLM since this was the only quantifiable local factor. The VLM in this case was derived from GNSS observations since the time the receivers started operating. The VLM rates computed from GNSS was assumed to be linear. The net SLR includes the global sea level increase. Manila Bay has the highest net SLR of 12.13 mm/year. The El Nido site has a high rate of 9.91 mm/year, but this is because the area is subsiding at a rate of -5.20 mm/year. It can be seen in this case that the actual SLR is 4.71 mm/year. Without the consideration of VLM, the SLR in El Nido appears to be accelerating. However, it is enhanced by the contribution of VLM. Cagayan de Oro is another site with a high rate of VLM. At a glance the sea level at the site is not influenced by El Niño. However, after adding VLM, the sea level is now about the same magnitude and trend of the neighboring TG sites in Tandag and Guiuan. Table 6 summarizes the net SLR from the 9 sites with collocated GNSS receivers.

The determination of net SLR is vital in future sea level projections and future coastal area inundations. As can be seen in some areas the VLM rate is higher than the SLR rate. The true SLR rate is contaminated by the contribution of VLM. It is prudent to not assume that the ground is static. Future coastal area inundation will be mapped more accurately if VLM should be considered as this varies from place to place. It is advisable to update the VLM rates from GNSS or InSAR every 5 years. Projection of sea level should go hand in hand with projection of ground motion especially on areas with high VLM rates.

Table 6. Net SLR from TG sites with collocated GNSS receivers

<i>Location</i>	<i>TGSL</i>	<i>VLM</i>	<i>Net SLR</i>	<i>Remarks</i>
Manila	13.13	-1.00	12.13	Probable contributions from other local factors
San Fernando	-1.01	-0.62	-1.63	Sea level fall (many data gaps in TG observations)
Cagayan de Oro	-1.05	-5.43	-6.48	Sea level fall due to effect of El Niño
Balanacan	0.12	-3.90	-3.78	Sea level fall due to effect of El Niño
Guiuan	-5.76	-0.91	-4.85	Sea level fall due to effect of El Niño
Cebu	1.28	-1.11	0.17	Sea level rise
El Nido	9.91	-5.20	4.71	High TGSL rate due to contribution from VLM
Davao	3.14	-1.59	1.55	Sea level rise

IV. CONCLUSIONS

The coastal sea level rise/fall depends on the strong influence of other local factors such as geographic location, climate pattern, ocean dynamics and varying geologic forms and settings. Based on the results, sea level measurements taken on sites facing the Pacific Ocean are directly affected by El Niño. The north and south side of the Philippines where currents from the Pacific Ocean flow through also manifest the influence of the said climate phenomenon. The occurrence of El Niño in 2009 to 2010 and 2015 to 2016, caused the sea level to fall. Specifically, the 2015 to 2016 El Niño was one of the three strongest events that were recorded. Since most of the TGs were installed in 2007 and 2008, the observed sea level for the short period of 12 or 13 years showed a downtrend.

In the south side of West Philippine Sea (WPS) in the Palawan area, warm water persists. Due to its location, water from the Pacific Ocean takes a longer time to flow through via the Luzon Strait route (northern Philippines). During El Niño, water from the Pacific Ocean is blocked by the water coming from the WPS in the Mindanao side, hence cold water is not entering. When southwest monsoon or “Habagat” comes, it warms the water more because it pushes warm water from the south and across the WPS to Palawan. Along with warm water, water also accumulates on the Palawan side, both contributing to the increasing sea level.

The sites with long period of observations (19 years or more) exhibit an increasing sea level trend that varies from 1.28 to 13.13 mm/year. The effect of tidal oscillations due to periodic climatic influence is dampened by the averaging. The effect of Pacific Decadal Oscillation (PDO) was not analyzed due to limited period of recorded data. The computed local SLR rates in the different study sites varies from each other and also varies with the global mean sea level rate of 3.4 mm/year. Thus, for determining sea level projections and coastal area inundations, it is wise to use the local SLR rates with long period of observations.

The computed sea level rise/fall rates from TGs correlated well with the rates from SA SSHs. A 0.96 correlation was computed between TGSL and 20 Hz SSH. Therefore, in the absence of installed TG in an area, SA 20 Hz can be used to estimate the sea level trend whenever available. Although ALES 1 Hz had an almost 19 years of assimilated data it had only 0.66 correlation with TG data. The reason is the few match points for comparison due to the low frequency of SSH data and the short period of observations from TGs. Nevertheless, ALES 1 Hz altimeter data can be used for long term analysis of sea level trend.

The MEaSURES Gridded SSH Anomalies with 28 years of assimilated data showed an uptrend for all sites. The advantage of this data is that almost all sites have SLR estimates due to interpolation done. However, users are cautioned to its use in the coastal. The SLR rates from MEaSURES gridded data ranges from 1.34 to 9.46 mm/year. For inference of sea level trend this data proved to be very valuable for analyzing the influence of periodic climate variability due to its long period of observations. The SA data is advantageous for sea level monitoring on sites that are open to sea or sites with little land mass in the surroundings that could contaminate the returned altimeter signal. From the results the water areas located in an inlet, channels and surrounded by islands showed doubtful trends. This is due to many data gaps and large data variability.

The local factor influencing the sea level rise/fall that was quantified in this study is the contribution of VLM. These rates were determined using PSInSAR technique and GNSS post processed solutions. The results from these two datasets have a high correlation of 0.89. This proves the viability of using PSInSAR for VLM determination sans the availability of GNSS receiver in the area. Almost all sites are undergoing land subsidence but those that should be noted are Cagayan de Oro and El Nido sites with more than 5 mm/year VLM rates. The VLM masked the true sea level magnitude and trend due to its influence.

Sea level rise in Manila Bay is accelerating at 13.13 mm/year. The usual attribution to this increase was due to land subsidence. The PSInSAR processing and GNSS solution showed that the TG area stable. The VLM rate at the Manila Bay TG site showed only very minimal contribution at -1 mm/year. Therefore, the net sea level rise is around 12.13 mm/year which is 4 times higher than the global MSL. This means that there are other factors contributing to the sea level increase. The initial results of hydrologic modeling done by the IM4Manila Bay Program showed an increase of discharge from river basins surrounding the bay. An increase in water surface runoff was also observed. The sea surface temperature from satellite sensors and the sea water temperature from in-situ measurements also showed an increasing trend. The measured sea water density/salinity is showing a decreasing trend. These manifestations explain the reasons why sea level is increasing in the bay. Other factors such as siltation,

excessive land reclamation and net water inflow/outflow in the mouth of the bay should be investigated further.

V. ACKNOWLEDGEMENT

The authors are grateful for the financial grant by the Department of Science and Technology Philippine Council for Industry, Energy and Emerging Technology Research and Development (DOST-PCIEERD) to the Coastal Sea Level Rise Philippines Project. Thank you also to the National Mapping and Resource Information Authority (NAMRIA) and Oscar M. Lopez (OML) Center for supporting the program.

REFERENCES

- [1] Ocean Topography from Space. 2017. Retrieved from <https://sealevel.jpl.nasa.gov/news/1532/why-am-i-here-a-brief-history-of-ocean-altimetry-and-why-its-the-most-important-mission-ever/>.
- [2] Nerem RS, Beckley BD, Fasullo JT, Hamlington BD, Masters D, Mitchum GT. 2018. Climate-change-driven accelerated sea-level rise detected in the altimeter era. Edited by Anny Cazenave. Proceedings of the National Academy of Sciences of the United States of America. PNAS. 2022-2025. <https://doi.org/10.1073/pnas.1717312115>
- [3] Passaro M, Cipollini P, Vignudelli S, Quartly GD, Snaith HM. 2014. ALES: A multi-mission adaptive subwaveform retracker for coastal and open ocean altimetry. Remote Sensing of Environment. 145:173-189. <https://doi.org/10.1016/j.rse.2014.02.008>
- [4] Rodriguez E. 1988. Altimetry for non-Gaussian oceans: Height biases and estimation of parameters. J. Geophys. Res. 93:14107–14120.
- [5] Thibaut P, Poisson J C, Bronner E, Picot N. 2010. Relative performance of the MLE3 and MLE4 retracking algorithms on Jason-2 altimeter waveforms. Marine Geodesy 33:sup1:317-335. doi: 10.1080/01490419.2010.491033
- [6] Roblou L, Lyard F, Le Henaff M, Maraldi C. 2007. X-track, a new processing tool for altimetry in coastal oceans. Geoscience and Remote Sensing Symposium, 2007. IGARSS 2007. IEEE International. doi: 10.1109/IGARSS.2007.4424016.
- [7] Brown G. 1977. The average impulse response of a rough surface and its applications. IEEE Trans. Antennas Propag. 25(1): 67–74.
- [8] Cipollini P, Snaith H. 2013. A short course on Altimetry. Cork, Ireland: National Oceanography Centre.
- [9] IHO. 2019. Hydrographic Dictionary.
- [10] Mercier F, Rosmorduc V, Carrere L and Thibaut P. 2010. Coastal and Hydrology Altimetry product (PISTACH) Handbook. Vol 4. Paris, France: Cent. Natl. d'Études Spat. (CNES).
- [11] OpenADB. <https://openadb.dgfi.tum.de/en/products/adaptive-leading-edge-subwaveform-retracker/>. Accessed June 2020 to May 2021.
- [12] Grgić M, Bender J, Bašić T. 2020. Estimating vertical land motion from remote sensing and in-situ observations in the Dubrovnik area (Croatia): A multi-method case study. Remote Sensing 12(21):3543. <https://doi.org/10.3390/rs12213543>.
- [13] Deng X, Featherstone WE. 2006. A coastal retracking system for satellite radar altimeter waveforms. J. Geophys. Res. Ocean 111 (C6).
- [14] Wöppelmann G, Marcos M. 2016. Vertical land motion as a key to understanding sea level change and variability. Rev. Geophys. 54(1):64–92.

- [15] Fenoglio-Marc L, Schöne T, Illigner J, Becker M, Manurung P, Khafid. 2012. Sea level change and vertical motion from satellite altimetry, tide Gauges and GPS in the Indonesian Region. *Mar. Geod.* 35(sup1):137–150.
- [16] Santamaría-Gómez A, Gravelle M, Wöppelmann G. 2014. Long-term vertical land motion from double-differenced tide gauge and satellite altimetry data. *J. Geod.* 88(3):207–222.
- [17] Geoscience Australia. Retrieved from <https://www.ga.gov.au/scientific-topics/positioning-navigation/geodesy/auspos> on June 2020 to May 2021.
- [18] Alaska Satellite Facility. Retrieved from <https://search.asf.alaska.edu/#/> on June 2020 to May 2021.
- [19] SARPROZ. Retrieved from <https://www.sarproz.com/> on June 2020 to May 2021.
- [20] Zlotnicki V, Zheng Q, Willis J. 2019. MEASUREs gridded sea surface height anomalies version 1812. Retrieved from podaac.jpl.nasa.gov on 01 May 2021.
- [21] Climate Data Guide. Retrieved from <https://climatedataguide.ucar.edu/climate> on 3 July 2021.
- [22] NASA. 2017. El Nino. Retrieved from <https://earthobservatory.nasa.gov/features/ElNino>.
- [23] Blunden J, Arndt DS. 2016. State of the climate in 2015. *Bull. Amer. Meteor. Soc.* 97(8). S1-S275.
- [24] Gordon AL, Huber BA, Metzger EJ, Susanto RD, Hurlburt HE, Adi TR. 2012. South China Sea throughflow impact on the Indonesian Throughflow. *Geop Res Lett.* 39:L11602. doi:10.1029/2012GL052021
- [25] CLS, SALT, CNES. 2014. Handbook for validation of altimeter data by comparison with TG measurement.
- [26] Reyes R, Bauzon A, Pasaje N, Alfante R, et al. 2022. Quantifying vertical land motion at tide gauge sites using permanent scatterer interferometric synthetic aperture radar and global navigation satellite systems solutions. *Spatial Information Research.* doi:10.1007/s41324-022-00431-y
- [27] Deguchi T, Kinugasa Y, Kurita K. 2011. Monitoring of land deformation using Terra SAR-X data around active fault in the Metro Manila, Philippines. FIG Working Week 2011: Bridging the Gap Between Cultures. Marrakech, Morocco.
- [28] INDRA, GISAT. 2021. Assessing changes in subsidence rates in the low Pampanga River basin and Manila area, Philippines.
- [29] De Lara P, Morado T. 2021. Estimation of absolute sea level rise in Marinduque using tide gauge measurements, GNSS, and InSAR techniques [undergraduate thesis]. Diliman(QC):University of the Philippines Diliman.
- [30] Rodolfo KS, Siringan FP. 2006. Global sea-level rise is recognised but flooding from anthropogenic land subsidence is ignored around northern Manila Bay, Philippines. *Disasters* 30(1):118–139.
- [31] Rodrigo C, Eco I, Rodolfo KS, Sulapas JJ, Rivera AM, Lagmay AMF, Falk A. 2020. Disaster in slow motion: Widespread land subsidence in and around Metro Manila, Philippines quantified by InSAR Time-Series Analysis. *JSM environmental Science and Ecology.*
- [32] Herrera E. 2021. The where, how and when of Manila Bay’s hydrodynamics. Manila Bay Conversations: Initial Findings and Assessment from the IM4ManilaBay Program.
- [33] The GHRSSST International Science Team. 2021. Retrieved from <https://www.ghrsst.org/ghrsst-data-services/products/> on Jan 2021.